Composite Yarns of Multi-walled Carbon Nanotubes with Metallic Electrical Conductivity

Lakshman K. Randeniya,[1*] Avi Bendavid1, Philip J. Martin[1], and Canh-Dung Tran [2,3]

[1] CSIRO Materials Science and Engineering PO Box 218, Lindfield, NSW 2070, Australia

[2] CSIRO Materials Science and Engineering PO Box 21, Belmont, VIC 3216, Australia

[3] Computational Engineering and Science Research Centre (CESRC), University of Southern Queensland, Toowoomba, QLD 4350, Australia

Abstract:

Unique macrostructures known as spun carbon-nanotube fibers (CNT yarns) can be manufactured from vertically aligned forests of multi-walled carbon nanotubes (MWCNTs). These yarns behave as semiconductors with room-temperature conductivities of about $5x10^2$ S cm^{-1}. Their potential use as, for example, microelectrodes in medical implants, wires in microelectronics, or lightweight conductors in the aviation industry has hitherto been hampered by their insufficient electrical conductivity. In this Full Paper, the synthesis of metal–CNT composite yarns, which combine the unique properties of CNT yarns and nano-crystalline metals to obtain a new class of materials with enhanced electrical conductivity, is presented. The synthesis is achieved using a new technique, self-fuelled electro deposition (SFED), which combines a metal reducing agent and an external circuit for transfer of electrons to the CNT surface, where the deposition of metal nano-particles takes place. In particular, the Cu–CNT and Au–CNT composite yarns prepared by this method have metal-like electrical conductivities (2–3 x 10^5 S cm^{-1}) and are mechanically robust against stringent tape tests. However, the tensile strengths of the composite yarns are 30–50% smaller than that of the unmodified CNT yarn. The SFED technique described here can also be used as a convenient means for the deposition of metal nano-particles on solid electrode supports, such as conducting glass or carbon black, for catalytic applications.

Keywords:

Carbon nanotubes, electrical conductivity, nano-composites, nano-crystalline materials, self-fuelled electro deposition.

1. Introduction

The unique properties possessed by hetero-structures of carbon nanotubes (CNTs) and metal nano-particles have potential applicability in a diverse field of industries [1,2]. The use of advanced electrically conducting CNT-composite yarns are well suited for use as, for example, low-impedance, high-capacity, more-robust microelectrodes in medical implants, low-resistance, high-strength wires in microelectronics, or light-weight conducting alternatives for complex systems in the aerospace industry [3,4]. Large cost savings and lower carbon footprints are also anticipated in the aviation and aerospace industry where the reduction of weight is a significant advantage. A number of laboratories, including ours, have demonstrated the production of CNT yarns from vertically aligned ''drawable'' multi-walled CNT (MWCNT) forests. Using concepts from textile production, a yarn is spun from vertically aligned MWCNT forests (Figure 1) [5–7]. These mechanically robust (tensile strengths of 1–2 GPa) and light-weight structures (~ a factor of 7 lighter than Cu) may now be produced on a large scale due to recent developments in spinning technologies. Continual improvements to the spinning processes and the preparation of well aligned MWCNT webs are being made in order to obtain yarns with better mechanical and physical properties [8].
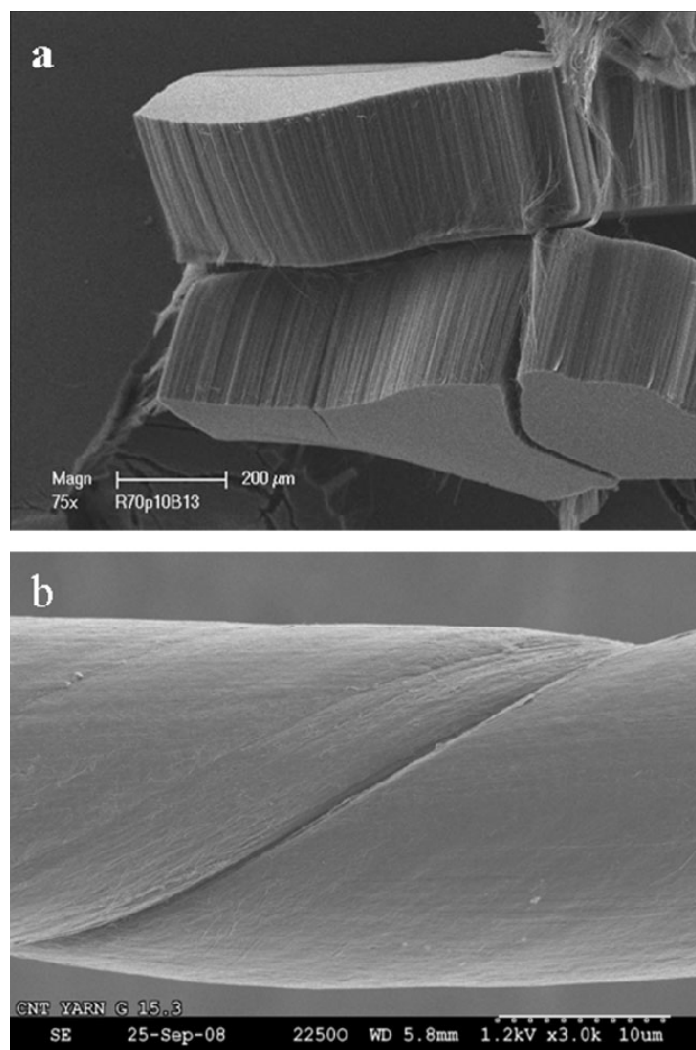
Figure 1. a) Drawable, vertically aligned MWCNT forest made in our laboratory by chemical vapor deposition using Fe catalysts and b) CNT yarn spun in our laboratory from a drawable MWCNT forest.

The electrical conductivity of MWCNT-based macrostructures, such as CNT yarns, is much lower than that of defect-free individual CNTs due to the presence of amorphous carbon and other impurities, which cause scattering and contact resistances [9–12]. Our measurements and previous measurements by Li et al [13] indicate that pristine CNT yarns prepared from long CNT fibers behave typically as semiconductors and have electrical conductivities in the range of 5–6 x 10^2 S cm^{-1} at room temperature. The utility of the CNT yarns can be facilitated by providing electrically conducting pathways in them. Post synthesis treatment of CNT yarn is one way of achieving this goal [13,14]. Choi et al.[15] showed that Au and Pt particles spontaneously deposited onto single-walled carbon nanotubes (SWCNTs) enhanced the electrical conductivity. Kong et al.[16] obtained hybrids of Au and SWCNTs with conductivities increased up to 2 x 10^3 S cm^{-1}. Li et al.[13] attempted incorporation of gold particles into MWCNT yarns using galvanic deposition in an ethanol solution of HAuCl4 with a view to increasing the electrical conductivity. However, the gold nano-particles were found to be sparsely distributed on the fibers and the increase in the electrical conductivity that could be attributed to the presence of gold particles on the nanofibers was less than 20%. In the present study, we describe a new technique, self-fuelled electro deposition (SFED),

which provides a contamination-free route for incorporating metals into CNT yarns and other CNT-based macrostructures, leading to composites with metal-like electrical conductivities. This method does not require the use of oxidative pre-treatments, which have the potential to damage the surface of the fibers.

2. Results and Discussion

Electrochemical deposition using an external current is widely used in industry and research for the deposition of metals on conducting, semiconducting, and insulating surfaces. The technique is less commonly used for the synthesis of noble metal nano-particles on CNTs [2]. Electroless deposition of metals, which does not require an external electrical current, is widely used in nanoscience, electronics, and membrane fabrication. The reduction of the metal ions is achieved by the use of hydrogen-containing reducing agents, such as hypophosphites, borohydrides, hydrazine, and formaldehyde [1]. Variations of the method include galvanic deposition and substrate-enhanced electroless deposition [15,17,18]. In the SFED technique described here, which has not been explored as a synthetic pathway for metals to date, electrons are spontaneously transferred from a sacrificial metal anode (the reducing agent, M_R) to the cathode substrate via an external circuit. The electromotive force is generated by the potential difference between the substrate and the M_R immersed in an electrolyte, which is a salt solution of the metal to be deposited (M_D). Therefore, an external voltage source is not needed for the deposition process. Unlike in the case of electroless deposition methods, there is no direct contact between the reducing agent and the substrate. In addition to the application shown here, where the method is used to produce hybrids of a metal and a CNT yarn, the SFED technique can also potentially be used as a convenient means for the deposition of metal nano-particles on solid electrode supports, such as conducting glass or carbon black, for catalytic applications.
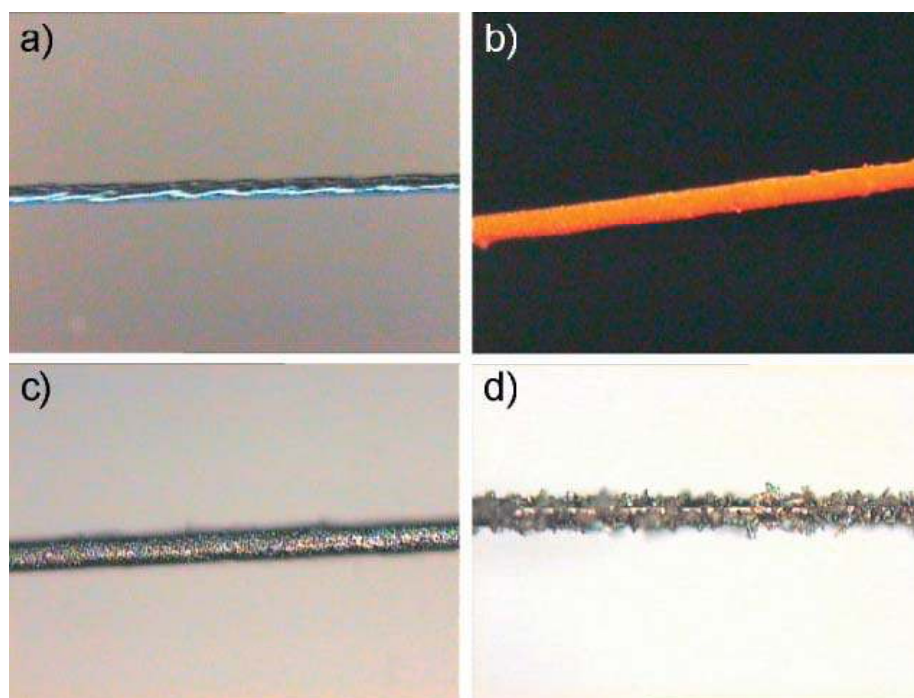

Figure 2. Optical microscopy images of a) pure CNT yarn, b) Au–CNT composite yarn, c) Pd–CNT-composite yarn, and d) Ag–CNT-composite yarn. Scale shown in Figure3 d applies to all panels. The Cu–CNT yarn hasamorphology similar to that of Au–CNT but with a pink/red color.

Optical images for the original CNT yarn and some metal–CNT yarns are shown in Figure 2. During the synthesis of the metal–yarn composites, the diameter of the yarn increased as the metal loading was increased. As discussed below, it was found that the metal deposited as nano-crystalline particles on the fibers of the yarn. Since CNT yarns are hydrophobic, we used ethanol in our solutions with a view to enhancing the penetration of the electrolyte into the yarn but this was not required. It is likely that some metal nano-crystalline particles are formed inside the composite yarns as well as that of the outer surface. Microscopic studies to confirm this were inconclusive and further studies are still underway. Attempts to incorporate Ag into CNT yarns resulted in the formation of micrometer-size aggregates on the outer surface (Figure 2d).
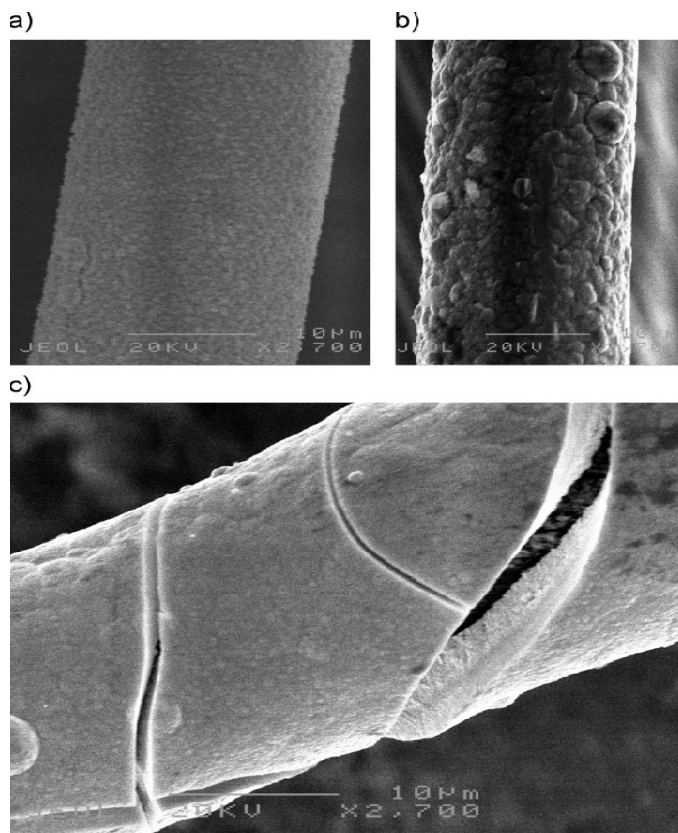

Figure 3. SEM images for metal–CNT yarns: a) Au–CNT, b) Cu–CNT, and c) Pt–CNT. Marked scales are 10μm.

Figure 3 shows scanning electron microscopy (SEM) images of composite yarns of CNTs with Au (Au–CNT), Cu (Cu–CNT), and Pt (Pt–CNT) prepared by the SFED technique. Figure 3a shows smooth distribution of gold in the Au–CNT yarns. This morphology is not affected by heating the sample up to $400^{o}C$. The surface of the Cu–CNT yarn, which is shown in Figure 3b, shows a distribution of particles that is less smooth in comparison to that of the Au–CNT yarn. Although the surface of the Pt-incorporated CNT yarn is much smoother (consisting of smaller nano-crystallites as discussed below), some discontinuities (micrometer-size cracks) can be observed on the surface (Figure 3c). These cracks become wider following heating at $400^{o}C$. For Pd–CNT yarns, such cracks start to appear only following heating in air at $400^{o}C$.

The crystallite sizes were estimated using the width of the X-ray diffraction (XRD) peaks and the Scherrer equation. In general, the crystallite sizes depended on the temperature of the electrolyte and the type of metal. The average crystallite sizes for Cu, Au, and Pd in the corresponding composites with CNT yarns formed at room temperature were found to be in the range of 20–40 nm. The lower average crystallite sizes correspond to lower metal loadings and the higher crystallite sizes to higher metal loadings (i.e., thicker samples). For Pt–CNT yarns, the average crystallite size of Pt was found to be 4–7 nm.

The Au–CNT and Cu–CNT wires prepared using the SFED technique withstood repeated ''tape tests'' without a change in resistivity or surface morphology. Here, general-utility tape was firmly attached to the composite wire and then removed, the resistivity was remeasured, and the surface was examined under an electron microscope to observe any damage. The Au–CNT and Cu–CNT wires were also successfully soldered onto circuit boards. Metal–CNT yarns prepared by SFED containing Pt and Pd were sufficiently robust for general handling and ultrasonic cleaning. However, surface damage occurred and the electrical resistance increased when tape tests were performed. Attempts to incorporate Ag into CNT yarns resulted in the formation of micrometer-size aggregates on the outer surface.

Mechanical measurements (stress versus strain) indicated that the pure CNT yarn (diameter: 13 mm) used in the current experiments had a tensile strength of ~1 GPa. For Au–CNT and Cu–CNT yarns with diameters of 23 mm, the tensile strength was found to be in the range of 500–650 MPa. This loss of tensile strength is a potential disadvantage of the hybrid material. In addition, the weights of the composite yarns are substantially higher than that of the pure CNT yarn. The density of the metal layers, as estimated from the weight measurements, increased with increasing diameter and then reached a plateau. For samples with an original diameter of 13 μm and then grown to composites with a diameter of 23 μm using different metals, the average densities of the metal layers were estimated from weight measurements to be 16.0 ± 0.6, 5.8 ± 0.4, 17.6 ± 0.6, and 8.6 ± 0.6 g cm^{-3} for Au, Cu, Pt, and Pd, respectively. The weight measurements indicated that, while the CNT yarn is about a factor of 7 lighter than that of Cu, the Cu–CNT yarn with a diameter of 17 μm is only a factor of 3 lighter than a Cu wire of similar dimensions and a Cu–CNT yarn with a diameter of 23 μm is only a factor of 2 lighter than a Cu wire with similar dimensions.

As mentioned earlier, during the synthesis phase, the diameter of the metal–CNT yarns increased as the metal loading was increased. In parallel, the measured electrical conductivity rose rapidly at first and then reached a plateau (Figure 4). For Cu–CNT yarns, the upper limit of the conductivity obtained in this study was $\sim 3 \times 10^5$ S cm^{-1} which is a factor of 600 larger than that of pristine CNT yarn. For Au–CNT yarns, the upper limit of the conductivity obtained was $\sim 2 \times 10^5$ S cm^{-1}. These values may be compared with pure copper and gold which have very high room-temperature electrical conductivities of 5.9×10^5 and 4.6×10^5 S cm^{-1}, respectively. The limiting electrical conductivities for Pd–CNT and Pt–CNT yarns were found to be 2×10^4 and 5×10^3 S cm^{-1}, respectively. For Pt–CNT composites, the limiting conductivity is a factor of 40 smaller than that of pure platinum metal. This large discrepancy in the limiting electrical conductivity between pure metal and the Pt–CNT composite could be a result of the lack of adhesion of Pt onto CNT fibers and the presence of structural defects (micrometer-size cracks) on the surface of the composite wire (see Figure 3c). The impact of these defects on the electrical conductivity was confirmed by heating experiments, in which a further decrease in conductivity was observed for Pt–CNT and Pd–CNT yarns due to the widening of these features.

In the use of the SFED process on a material with a low electrical conductivity, such as a CNT yarn, the nucleation occurs first near the galvanic contact and then proceeds further

down the yarn as the electro-active area increases. In the case of Cu and Au, the nucleation and deposition rates are such that uniformly thick metal layers are formed more than 10 cm across the yarn from the galvanic contact. This is because Cu and Au bond strongly to the CNT fibers via van der Waals intermolecular forces at the initial stage of deposition. As a result, as the metal deposits, the electrical conductivity of the composite yarn increases and the electro-active area extends rapidly to regions further and further away from the galvanic contact. In contrast, in the case of Ag, as seen in the images shown earlier in Figure 2, discontinuous metal aggregates are formed closer to the galvanic contact instead of a uniform film across the yarn. Metal layers tend to grow thicker closer to the galvanic contact and the deposition terminates just 2–3 cm away from the galvanic contact. These effects can be attributed to the poorer penetration and adhesion of Ag atoms to the CNT fibers (metal layers can be easily detached from the yarn using an ultrasonic bath) in comparison to that of Au and Cu. As a result of poor adhesion, the electrical conductivity of the Ag–CNT composite yarns does not increase and the electro-active area remains confined to the near vicinity of the galvanic contact. The cases for Pt–CNT and Pd–CNT yarns can be considered to fall in the middle of the above two cases.
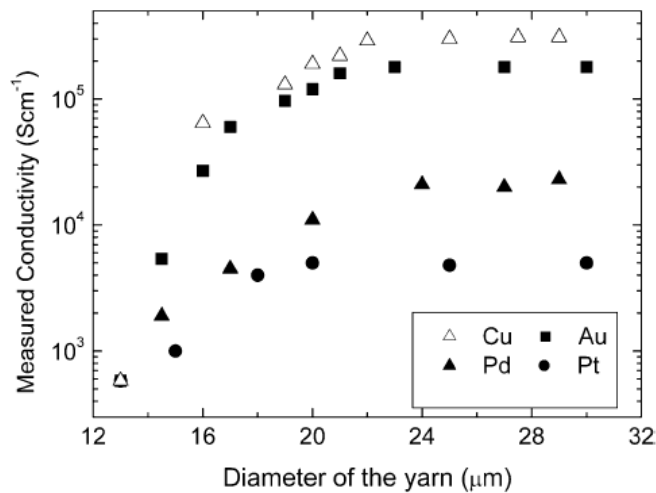

Figure 4. Variation of the conductivity as a function of metal loading (measured by the diameter) for metal–CNT-composite yarns. The average diameter of the pure CNT yarn is 13μm.

Figure 5 shows the relationship between the temperature and resistivity of the pure CNT yarn and the metal–CNT yarns. The pure CNT yarn behaves as a typical semiconductor, with the resistivity increasing as the temperature decreases. Fitting the conductivity data to an electron-tunnelling-conduction model and to a variable-range electron-hopping model indicated that neither mechanism can explain the charge conduction in the pristine CNT yarns for the entire temperature range studied here. As observed by Li et al. [13] data taken at temperatures above 50K are more consistent with the model for three-dimensional electron hopping than the model for tunnelling conduction.

As seen in Figure 5, the Au–CNT and Cu–CNT yarns show a typical metal-like dependence of electrical resistivity on temperature. The estimated temperature coefficient of the resistivity is 3.2×10^{-3} K^{-1} for the Au–CNT yarns and 3.9×10^{-3} K^{-1} for Cu–CNT yarns. The corresponding values for pure gold and pure copper are 3.2×10^{-3} and 3.9×10^{-3} K^{-1}, respectively. This confirms the prominent role of nano-crystalline gold and copper in conducting electricity through the corresponding composite yarns. The results clearly show that Au–CNT and Cu–CNT yarns have unique properties in comparison to other metal–CNT

yarns studied here. The mechanical robustness and the nature of the electrical conductivity are particularly remarkable. The Au and Cu particles are more strongly attached to the CNT fibers in comparison to other metals studied here. The high ductility of Au and Cu minimizes the development of structural defects and provides the continuity of particle interconnectedness through these yarns.
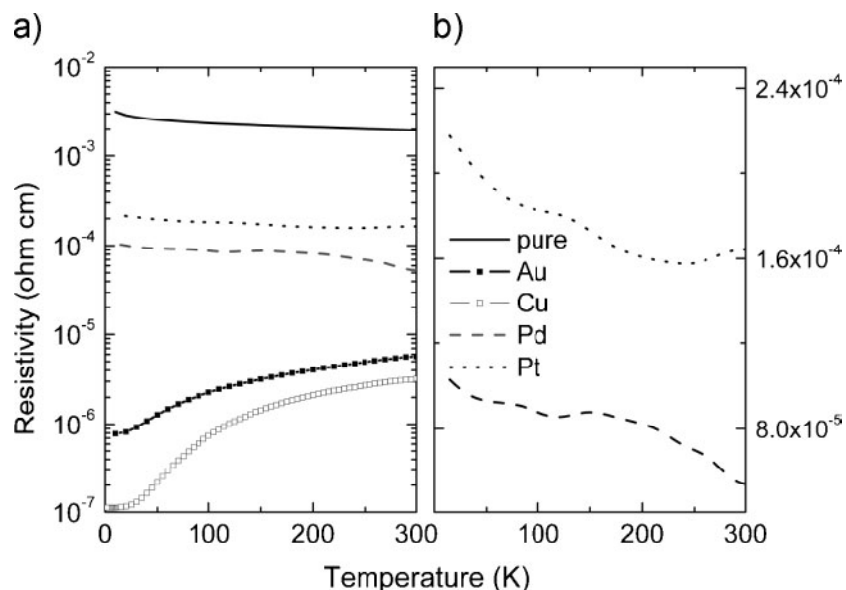

Figure 5. Temperaturedependencesoftheresistivity fora)Au–CNT-,Cu– CNT-, Pd–CNT-, and Pt–CNT-composite yarns and original CNT yarns on a log scale and b) the Pd–CNT and Pt–CNT yarns on a linear scale.

As seen in Figure 5, the Pt–CNT yarn also shows a general trend in the temperature dependence of the resistivity similar to that of pure CNT yarn; however, the influence of temperature is smaller for the case of Pt–CNT yarn. The Pd–CNT yarns shows the behavior of a semiconductor with distinct temperature regimes where the resistivity is relatively constant. Although there is a factor-of-forty reduction in the room-temperature resistivity for a Pd–CNT yarn in comparison to a pure CNT yarn, the temperature dependence of the resistivity still resembles a semiconductor-like material. For both Pt–CNT and Pd–CNT yarns, there are temperature regimes of metal-like behavior, where the resistivity increases with temperature. Further investigations are required to understand the interplay between the metallic and semiconducting behaviors of the composite yarns.

The XRD data indicates that the lattice structure for Au and Cu polycrystalline films formed on the CNT fibers is face centered cubic, which is the same as that of the bulk metals. The resistivity of thin metal films and wires is highly sensitive to their polycrystalline structure and surface morphology because grain boundaries and surfaces provide additional scattering sites compared to bulk materials. Although there is evidence that some increase in electrical conductivity in Cu–CNT and Au–CNT yarns occurs initially via penetration of metal particles into the CNT yarn, we modelled that the bulk of the electrical conductivity occurs through the metal shell formed around the CNT yarn. Using this model, we estimated the conductivity of the deposited metal films on Cu–CNT and Au–CNT yarns shown in Figure 4 to be approximately 70% of the corresponding bulk metal. We also note that the temperature dependence of the resistivity of the composites is similar to that of the bulk metal. The lower conductivity observed in the polycrystalline metal films formed on the composites can be attributed to the presence of grain boundaries [19, 20]. The surface scattering, which can be important for metal nano-wires, is much less important for metal–CNT composite wires since

the thickness of the metal film is much greater than the electron mean free paths for the corresponding metals. The crystal structure for Pt and Pd layers were also found to be the same as that found for bulk materials. In these cases, as discussed earlier, large-scale structural deformities contribute to the observed electrical conductivity being much lower than that of the corresponding bulk metal.

3. Conclusions

CNT-based macrostructures, such as CNT yarn and CNT webs produced in our laboratories, have certain advantages and direct application routes over powder-based materials. The new electro deposition technique described here, SFED, is particularly relevant for metal-nano-particle incorporation into macrostructures of CNTs and other materials. The synthesis of electrically conducting hetero structures of CNT yarns and nano-crystalline metals is now possible, paving the way for their potential use in certain industrial and research applications. Further research is needed to reduce the loss of tensile strength and to minimize the increase in weight in the metal–CNT composite yarns in comparison to that of pure CNT yarns. SFED also allows the direct deposition of pristine nano-crystalline noble metals onto suitable electrode supports made of high surface area nanostructures for studies in catalysis, membrane technologies, and other relevant areas.

4. Experimental Section

CNT yarns were prepared from vertically aligned CNT forests grown on Si/SiO2 substrates with Fe as a catalyst using a chemical vapour deposition method [21]. The lengths and outer diameters of the CNTs were ~300–400 µm and ~7.5–8.5 nm, respectively. The yarns were prepared by spinning methods described earlier [6,8]. The diameters of the original CNT yarns used in the present experiment were 13, 20, and 27 µm. Pre-treatment of the substrate surface using methods such as ozonolysis and submerging in strong acids prior to the deposition of metal particles onto CNTs was not used. Figure 6 shows an SFED configuration used for the preparation of nano-crystalline gold and CNT (metal–CNT) composite yarns. A CNT yarn is immersed in an aqueous solution (typically 10×10^{-3} M) of the salt of the metal to be deposited (M_D). Ethanol solutions of the salt can also be used but the deposition occurs at a lower rate. The two ends of the yarn are connected electrically to the reducing metal anode, MR, which has a lower reduction potential than M_D. Examples for combinations of M_D, M_R, and suitable salts of M_D are shown in Table 1. Connecting both ends to the reducing metal aided smooth, uniform deposition along the length of the CNT yarn. The CNT yarn can be loosely wrapped around a tubular glass stent, which allows all surfaces of the yarn to be in direct contact with the electrolyte. The ceramic frit prevents any insoluble particles formed at the anodes from moving to the chamber containing the substrate. The deposition process for CNT yarns commences when the galvanic connection is short circuited and stops when the concentration of either the reducing agent or the metal ion reaches zero. Hence, a desired composition for the resulting Au–CNT yarn can be achieved by adjustment of the concentration of the $HAuCl_4$ solution and exposure time.
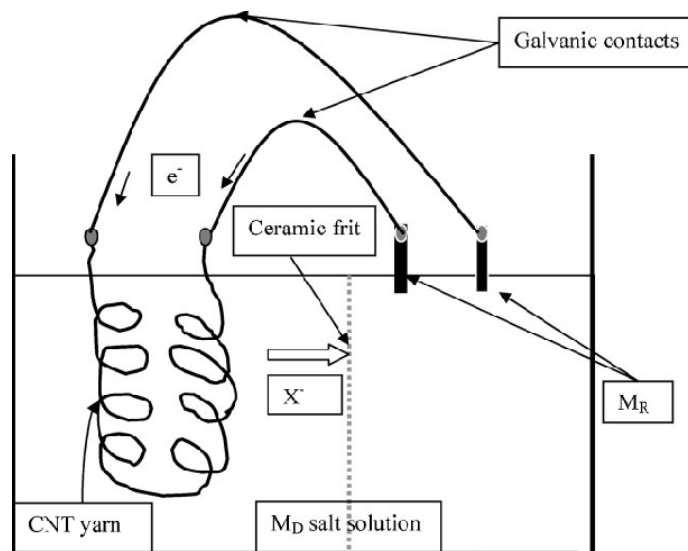
Figure 6. SFEDarrangement usedfor incorporating metal particles into a CNT yarn. Composite yarns with lengths of up to 50 cm were prepared under normal laboratory conditions. Slow stirring was carried out with a magnetic bar. X is the anion carrying negative charge (e.g., Cl).

There is a competing reaction for SFED known as displacement deposition, in which the reduction of $HAuCl_4$ occurs on the surface of the Cu anode itself. For this reason, M_R should only be in contact with the solution during the deposition period. The impact of displacement deposition may be minimized by the use of sufficiently thin samples of M_R and by exposing smaller surface areas of MR to the electrolyte. XRD studies used a P analytical X 'Pert Pro diffractometer with an X'cellerator multichannel detector and a real-time multiplier strip. SEM measurements were performed using a JEOL JSM 5400LV spectrometer. The resistivity of the yarns and the temperature dependence of the resistivity were measured using a four-point Quantum Design materials property measurements system.

Acknowledgements

References

[1] X. Peng, J. Chen, J. A. Misewich, S. S. Wong, Chem. Soc. Rev. 2009, 38, 1076–1098.

[2] G. Wildgoose, C. Banks, R. Compton, Small 2006, 2, 182–193. [3] R. H. Baughman, A. A. Zakhidov, W. A. de Heer, Science 2002, 297, 787–792.

[4] G. G. Wallace, S. E. Moulton, G. M. Clark, Science 2009, 324, 185–186.

[5] K. Jiang, Q. Li, S. Fan, Nature 2002, 419, 801–803.

[6] M. Zhang, K. R. Atkinson, R. H. Baughman, Science 2004, 306, 1358–1361.

[7] Y. Li, I. A. Kinloch, A. H. Windle, Science 2004, 304, 276–278.

[8] C. D. Tran, W. Humphries, S. M. Smith, C. Huynh, S. Lucas, Carbon 2009, 47, 2662–2670.

[9] S. N. Song, X. K. Wang, R. P. Chang, J. B. Ketterson, Phys. Rev. Lett 1994, 72, 697–700.

[10] A. Bachtold, M. Henney, C. Terrier, C. Strunk, C. Schonenberger, J. P. Salvetat, J. M. Bonard, L. Forro, Appl. Phys. Lett 1998, 73, 274–276.

[11] H. Dai, E. W. Wong, C. M. Lieber, Science 1996, 272, 523–526. [12] C. Berger, Y. Yi, Z. L. Wang, W. A. de Heer, Appl. Phys. A 2002, 74, 363–365.

[13] Q. Li, Y. Li, X. F. Zhang, S. B. Chikkannanavar, Y. H. Zhao, A. M. Dangelewicz, L. X. Zheng, S. K. Doorn, Q. X. Jia, D. E. Peterson, P. N. Arendt, Y. T. Zhu, Adv. Mater 2007, 19, 3358–3363.

[14] R. S. Lee, H. J. Kim, J. E. Fischer, A. Thess, R. E. Smalley, Nature 1997, 388, 255–257.

[15] H. C. Choi, M. Shim, S. Bangsaruntip, H. Dai, J. Am. Chem. Soc 2002, 124, 9058–9059.

[16] B. S. Kong, D. H. Jung, S. K. Oh, C. S. Han, H. T. Jung, J. Phys. Chem. C 2007, 111, 8377–8382.

[17] L. A. Porter, H. C. Choi, A. E. Ribbe, J. M. Buriak, Nano Lett. 2002, 2, 1067–1071.

[18] L. Qu, L. Dai, J. Am. Chem. Soc 2005, 127, 10806–10807.

[19] A. F. Mayadas, M. Shatzkes, J. F. Janak, Appl. Phys. Lett 1969, 14, 345–347.

[20] J. W. C. De Vries, Thin Solid Films 1988, 168, 25–32.

[21] X. B. Zhang, K. L. Jiang, C. Teng, P. Liu, L. Zhang, J. Kong, T. H. Zhang, Q. Q. Li, S. S. Fan, Adv. Mater 2006, 18, 1505–1510.